



International Journal for Innovative Engineering and Management Research

A Peer Reviewed Open Access International Journal

www.ijiemr.org

COPY RIGHT



ELSEVIER
SSRN

2019IJIEMR. Personal use of this material is permitted. Permission from IJIEMR must be obtained for all other uses, in any current or future media, including reprinting/republishing this material for advertising or promotional purposes, creating new collective works, for resale or redistribution to servers or lists, or reuse of any copyrighted component of this work in other works. No Reprint should be done to this paper, all copy right is authenticated to Paper Authors

IJIEMR Transactions, online available on 4th Sept 2019. Link

[:http://www.ijiemr.org/downloads.php?vol=Volume-08&issue=ISSUE-09](http://www.ijiemr.org/downloads.php?vol=Volume-08&issue=ISSUE-09)

Title **CONTROL OF A 3Ø CONVERTER FOR A PV CHARGING STATION**

Volume 08, Issue 09, Pages: 503–515.

Paper Authors

K PRAVARSHA, G BHAVYA SREE, P NIHARIKA

Anu Bose Institute of Technology K.S.P Road, New paloncha, Bhadradi Kothagudem, Telangana, India



USE THIS BARCODE TO ACCESS YOUR ONLINE PAPER

To Secure Your Paper As Per **UGC Guidelines** We Are Providing A Electronic Bar Code

CONTROL OF A 3Ø CONVERTER FOR A PV CHARGING STATION

K PRAVARSHA¹, G BHAVYA SREE², P NIHARIKA³

^{1,2,3}UG Students, Dept. of Electrical and Electronics Engineering Anu Bose Institute of Technology KSP Road, Newpaloncha, BhadradiKothagudem, Telangana, India.

pravarshakasarla@gmail.com¹, bhavyasreeg22@gmail.com², kasihussain55@gmail.com³

Abstract: -Cross breed help converter (HBC) has been proposed to supersede a dc/dc boost converter and a dc/cooling converter to diminish change organizes and trading mishap. In this paper, control of a three-arrange HBC in a PV charging station is organized and attempted. This HBC interfaces a PV system, dc structure with cross breed module electrical vehicle (HPEVs) and a three-arrange cooling grid. The control of the HBC is proposed to recognize most outrageous power point following (MPPT) for PV, dc transport voltage rule, and cooling voltage or open power rule. A test bed with power devices trading nuances is worked in MATLAB/SimPower systems for endorsement. Amusement results demonstrate the reasonableness of the organized control designing. Finally lab preliminary testing is directed to display HBC's control execution.

Index Terms: Plug-in Hybrid Vehicle (PHEV), Vector Control, Grid Connected Photovoltaic (PV), Three Phase Hybrid Boost Converter, Maximum Power Point Tracking, Charging Station.

1. INTRODUCTION

The common and monetary focal points of PHEV lead to the extension in number of age and usage [1]. The U.S. Division of Energy measures more than one million PHEVs will be sold in the U.S. during the next decade [2]. Research has been driven on structure up a charging station by organizing a three-arrange cooling network with PHEVs [3]–[5]. The relationship of different PHEV chargers' topologies and frameworks are evaluated in [1][6]. Regardless, a gigantic scale passageway of PHEVs may incorporate more weight the system during charging periods. As needs be, blaming stations for PV as an additional power source turns into a reachable game

plan. For PV charging stations, [7] proposed designing and controllers. The charging the officials is made in [8] by considering the structure's stacking limit. For this sort of structures, it requires controlling at any rate three differing power electronic converters to charge PHEVs. Each converter needs an individual controller which assembles multifaceted nature & influence incidents of the structure. Along these lines, it is basic to look into multi-port converter to reduce the amount of changing over stages. The objective of the article is to realize such a multi-port converter in a PV charging station for PHEVs and plan the controller.

A. Related Works

To decrease the amount of trading stages, the inverse Watkins-Johnson methodology is proposed in [9] by giving force simultaneously to dc and cooling loads. Single-phase and three-time of hybrid help converters (HBC) that can consolidate a dc power source, dc weights and cooling loads for a microgrid are proposed in [10] and [11], independently. Late research in [12] in like manner suggests that a cross breed single-arrange converter can be associated in network related applications. All past research on HBC controller structure [10]–[12] expect that the cream converter is related with a solidified dc voltage source. From this time forward, the limit of most outrageous power point following (MPPT) for PV systems isn't yet made for HBC. Regardless of the way that MPPT figuring exists in the composition, the application is on a very basic level for a dc/dc converter or a dc/cooling converter. Use of MPPT in HBC has not been analyzed. This utilization is unquestionably not a frivolous issue since it requires a concentrated appreciation on HBC trading framework and the coordination of MPPT work and the vector control work.

B. Our Contributions

This paper proposes control plan and power the board for a PV charging station for PHEV by usage of a three-arrange HBC. The PV charging station charges PHEVs using power from PV just as the climate control system structure. The three-arrange HBC facilitates three rule parts of the structure: PV, PHEV and the grid control

setup will be presented in detail. The control will engage PV most extraordinary power point following MPPT dc voltage control rule for PHEVs. Our duties lie in two points. The fundamental duty is exhibiting of a PV charging station reliant on a three-arrange HBC that directs PV bunches, PHEVs, and an utility grid. This story topology of PV charging station, the extent that writers could know, has not yet been found in the composition. The upside of the HBC based PV charging station is the reduction of the amount of force change stages and incidents. The current PV charging station requires controlling in any occasion three converters including a dc bolster converter for MPPT figuring, a three-arrange dc/cooling inverter, and a dc converter for battery's charging [15]. Or maybe, the HBC arranges the primary dc bolster converter and the dc/cooling three-organize inverter into a singular structure. The consequent duty is the arrangement of the HBC controller. Existing controllers for HBC [10][12] have avoided MPPT work since the dc data side is acknowledged as a solidified dc voltage in the recently referenced research. In our assessment, we consider the nuances related to the PV further executed MPPT computation in a HBC.

C. Organization of the Paper

The rest of the paper is dealt with as seeks after. The topology and suffering state characteristics of the 3-arrange HBC are depicted in Section II. A balanced PWM using five reference signals (three-arrange cooling voltage sign and positive and negative dc signals) is in like manner shown

around there. MPPT count, arrange shot circle (PLL), vectorcontrol and the battery charging plan are presented in Section III. Zone IV presents logical examination results to test the show of the controller by methods for reenactment coordinated in MATLAB/Simpowersystems. Portion V gives the test outcomes which is recognized using LabView-FPGA module planning with National Instruments Single Board RIO-9606.

II. THREE-PHASE HBC-BASED PV CHARGING STATION TOPOLOGY AND OPERATION

A three-organize HBC uses indistinct proportion of changes from a two-level voltage source converter (VSC). In any case, the HBC can comprehend both dc/dc change and dc/ac change. As a relationship, Fig. 1 exhibits the standard PV charging station where a dc/dc help converter and a three-organize VSC are used to arrange the PV structure, the PHEVs and the climate control system grid. A three-organize HBC replaces the two converters: the dc/dc booster converter and the dc/ac three-organize VSC to reduce the imperativeness change stages and the influence disasters of the PV charging station. Fig. 2 exhibits the HBC based PV charging station's topology. The crucial pieces of the course of action of the PV charging station involve PV display, three-organize bidirectional HBC, cooling structure, off-board dc/dc converter, and PHEV's batteries.

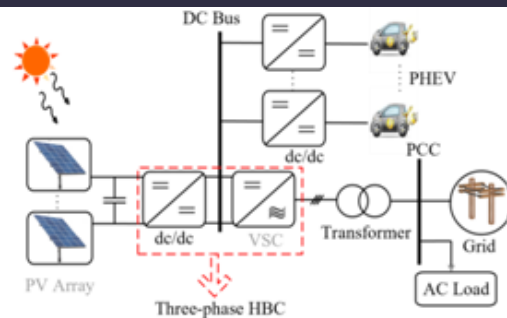


Fig. 1. Architecture configurations of a PV charging station. The conventional topology includes a dc/dc converter and a dc/ac VSC. These two converters will be replaced by a three-phase HBC.

To design the control of a PV charging station, it is essential to grasp the movement of a three-organize HBC. Point by point action of a HBC can be found in [10], [11], [16]. Here a short depiction is given. The system is made out of a PV display, a dc structure, a three-organize cooling structure, and the interfacing three-organize HBC as showed up in Fig. 2. The PV side consolidates a tremendous inductance to achieve tireless condition & capacitance to reduce the voltage swell. The dc side joins a diode, a dc transport for PHEV affiliation, a dc capacitor to get rid of the yield current swells, an off-board unidirectional restricted dc/dc converter, and PHEV batteries. The climate control system structure fuses a three-organize LC channel, a phase up transformer, and the motivation behind fundamental coupling (PCC) transport that interfaces the PV station to the essential cross section. The PV display is made out of partner game plan cells and parallel strings. Each PV cell has express characteristics depending upon the sort and organizing criteria. PV models depend generally on Shockley diode condition [17], [18]. PV can

be shown as a photon-made current source in parallel with a two-diode system and a shunt resistor, R_{sh} , similarly as in game plan with a course of action resistor, R_s . The numerical states of two-diode PV cell are given in [17]. A shot at two modes which are "on" and "off" states. Customary VSC is taken a shot at "dynamic" and "zero" modes where the yield cooling power can have a value or zero. The three-arrange HBC organizes the operational times of a VSC and a dc/dc converter into three principal modes. The standard three intervals join a shoot-through mode, a working mode (An), and a zero mode (Z). A couple of doubts are considered to all the more probable layout the suffering state action of the three-organize HBC. In the first place, the structure is believed to be lossless where the damping segments proportionate zero. Second, the voltage drop on the diode is close to nothing so it will in general be dismissed. Next the operational technique for the three-phase HBC is filled in as an inverter where the power streams from the PV into the cross section. It is seen that the three stage HBC can be worked at converter or inverter reliant on the heading of force stream. Finally, the diode current is endless during the dynamic stage. The suffering state the forced air system side are given as seeks after.

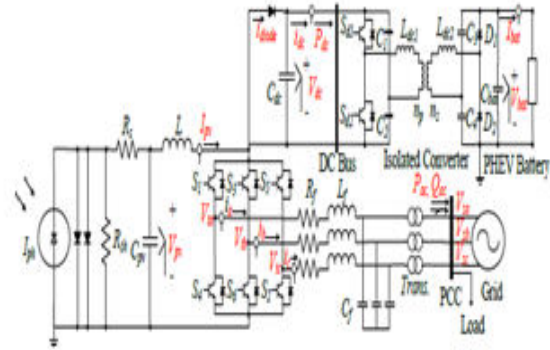


Fig. 2. Topology of the three-phase HBC-based PV charging station.

A. Modified PWM

It is referenced in Section II that the three-stage HBC is worked at three primary interims which are incorporated between lift converter and VSC's stages. Regular sinusoidal PWM and dc PWM are not suitable to work the exchanging conditions of three-stage HBC. Rather than independently controlling the dc and air conditioning yields utilizing the switches of three-phase HBC, an altered PWM is connected to control two yields simultaneously as appeared in Fig. 3. It is prescribed to embed the shoot-through stage inside the zero mode where the yield air conditioning force equivalent is zero in this stage [20]. frameworks while the current to the air conditioner framework is zero. At last, during the dynamic mode, current will stream into the air conditioner system. The conduct of the open-circle control conspire for exchanging conditions of the three-stage HBC is appeared in Fig. 3 when the reference for the stage voltages are connected as $V_a > V_b > V_c$. The shoot-through activity happens when the positive sign V_{st} is lower than bearer signal (stage C is shoot through

with S5 and S2) and when the negative sign Vst is more noteworthy than the transporter signal (stage An is shoot-through with S1 and S4 on). Shoot through occurs at the stages with the most astounding voltage or least voltage. In Fig. 3, stage An and Phase C are the stages with shoot-through periods. Altered PWM directs the exchanging states by controlling five sign which are three-stage air conditioning signals Va, Vb, Vc, and dc signals Vst ($V_{st} = 1 - D_{st}$), and $-V_{st}$. The air conditioner controlling sign Va, Vb, and Vc are constrained by adjustment file Mi just as stage points while the dc signals $+V_{st}$, and $-V_{st}$ are directed obligation proportion D_{st} . The upside of utilizing altered PWM is that both dc and air conditioning yields can be balanced.

III. CONTROL OF PV CHARGING STATION

This segment gives a nitty gritty clarification on the system and controller of the HBC based PV charging station. From the enduring state relationship in (2) three-stage HBC uses D_{st} to support the PV voltage while the tweak list Mi controls the air conditioner voltage V_t 's extent. Likewise, the point of the three-stage air conditioning voltage V_t can be changed in accordance with accomplish dynamic power and receptive power guideline. At the point when the air conditioner voltage is adjusted and the air conditioner framework is symmetrical, the total three-stage prompt power is consistent at steady state. Consequently, normal intensity of the air conditioner side equivalents to the net power at the dc side ($P_{ac} = P_{pv} - P_{dc}$). The principle

control squares are utilized to control the three-phase HBC MPPT, stage bolted circle (PLL) and vector control as appeared in Fig. 4. Each square will be portrayed by a subsection. The charging calculation of the off-board segregated dc/dc converter will likewise be tended to in this area.

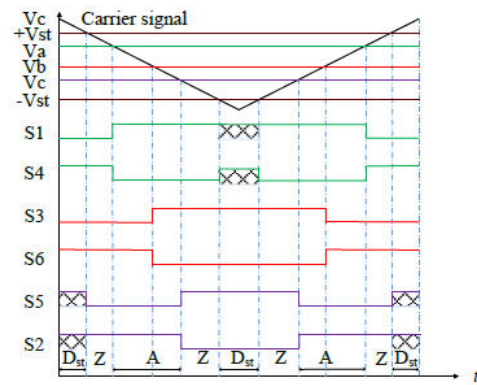


Fig. 3. A modified PWM for the three-phase-HBC. Shoot-through occurs when both switches are closed. ST, A, and Z are shoot-through, active, and zero periods, respectively.

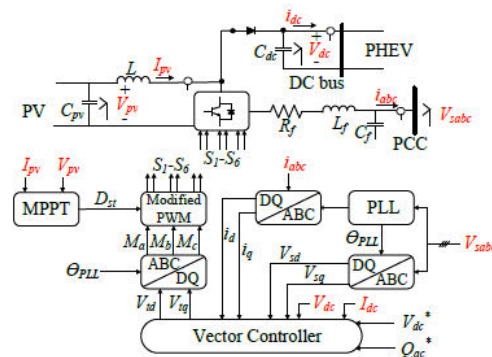


Fig. 4. Control blocks of the HBC-based PV charging station.

IV. SIMULATION RESULTS

Case studies for a PV charging station using a three phase HBC with the proposed control are conducted in MATLAB/SimSystems environment. The system parameters and PV data are given in Table I. The data for the PV model are based on PV array type Sunpower SPR-E20-327. The V-I and PV curves for different irradiance values are shown

in Fig. 5. The battery parameters of Chevrolet Volt and Nissan Leaf are used to represent the batteries of PHEV [6][35][36]. Five case studies are conducted to evaluate MPPT and vector control as well as to illustrate the operation modes of the PV charging station.

A. Case 1: Performance of the Modified Incremental Conductance-PIMPPPT

The objective of this contextual investigation is to approve the exhibition of the adjusted MPPT utilizing gradual conductance PI calculation. As per Fig. 5, the greatest PV power is 100 kW when the PV cluster produces 273.5 V at 1 kW/m² sun based irradiance. Fig. 14 demonstrates the presentation of MPPT when the framework liable sunlight based irradiance variety. The dc voltage V_{dc} and the PV voltage V_{pv} are related dependent on the obligation cycle proportion D_{st} that is produced from MPPT. The job of vector controller is to keep the dc voltage V_{dc} at its reference esteem 350 V and supply receptive capacity to the air conditioner framework. The job of MPPT calculation is to modify the obligation cycle proportion D_{st} and thusly alter the PV yield voltage V_{pv} so that the PVs are working at the most extreme power removing point. Fig. 14 gives the exhibition of MPPT dependent on four distinct interims. From 0–0.5 seconds the sun irradiance is 0.9 kW/m² and the MPPT control isn't enacted. The output PV power supplies roughly 70 kW. At $t=0.5$ seconds, MPPT is actuated, the obligation cycle proportion is diminished and the PV voltage is improved. This thus improves the PV power yield to be 90 kW. Note that whether the MPPT is on or off, V_{dc} is kept at 350 V.

TABLE I
SYSTEM PARAMETERS

Parameters		Parameters	
PV	$V_{oc} = 65.1$ V	AC	$V_{grid}(L-L) = 20$ kV
	$V_{mpp} = 54.7$ V		$\omega = 377$ rad/s
	$I_{sc} = 6.46$ A		$S = 100$ kVA
	$I_{mpp} = 5.98$ A		$V_l(L-L) = 208$ V
	$R_{sh} = 298.531$ Ω		$R_f = 2$ m Ω
	$R_s = 0.369$ Ω		$L_f = 125$ μ H
			$C_f = 150$ μ F
DC	$V_{dc} = 350$ V	Control	$K_{pi} = 0.625$ Ω
	$L = 5$ mH		$K_{ii} = 10$ Ω/s
	$C = 12000$ μ F		$K_{pv} = 0.24$ Ω^{-1}
	$Load = 100$ kW		$K_{iv} = 300$ Ω^{-1}/s
	$L_{dc} = 10$ mH		$K_{pvd} = 0.001$
	$C_{dc} = 100$ μ F		$K_{ivdc} = 25$
			$K_{iivdc} = 0.001$
			$K_{iivdc} = 3$
Chevy	# of Cells: 200	Nissan	# of cells: 160
	$V_{cell} = 1.25$ V		$V_{cell} = 1.875$ V
	$Q_{energy} = 16$ kWh		$Q_{energy} = 24$ kWh
	Type: Li-Ion		Type: Li-Ion

At $t=1$ second and $t=1.5$ seconds, the sun irradiance increments & diminishes. Because of the MPPT control, the ideal PV yield voltage is kept at the ideal level. Further, the PV yield power tracks the most extreme point at every irradiance level. Fig. 14 approves the great following presentation of MPPT when diverse sun based illuminations are connected to the PV. The reproduction results likewise demonstrate that the vector controller can manage the dc voltage at 350 V and reject unsettling influences.

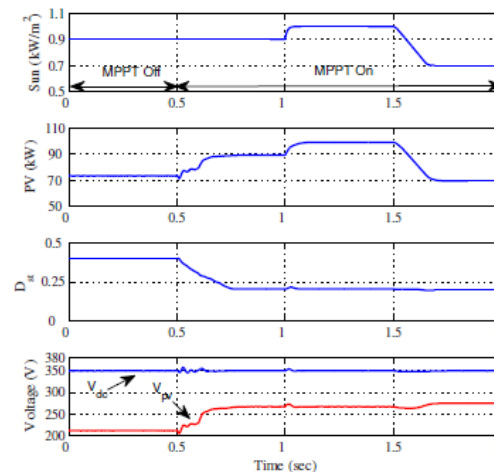


Fig. 14. Performance of a modified IC-PI MPPT algorithm when solar irradiance variation is applied.

B. Case 2: Performance of the DC voltage controller

The benefits of actualizing the three-stage HBC on PV charging station is its ability to supply dc and air conditioning power at the same time. The fundamental goal of a PV charging station is to supply constant dc capacity to electric vehicles. Case 2 examines the capacity of the proposed controller to furnish consistent dc voltage with PV control variety and MPPT control status change. As a correlation, a framework with dc voltage control handicapped is likewise reenacted. For this framework, the referenced-pivot current is kept steady.

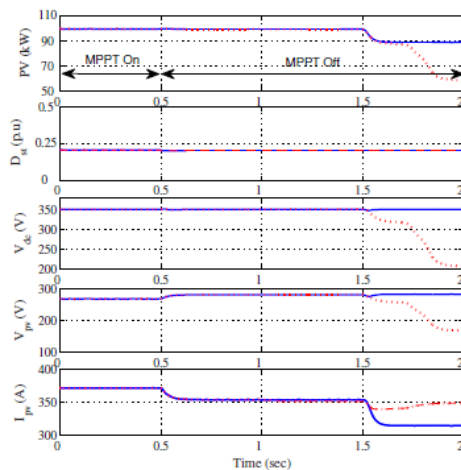


Fig. 15. Performance of the dc voltage control in the vector control. The solid lines represent the system responses when the dc voltage control is enabled. The dashed lines represent the system responses when the dc voltage control is disabled.

The strong lines speak to the framework reactions when the dc voltage control is empowered. The dashed lines speak to the framework reactions when the dc voltage control is disabled. Fig. 15 demonstrates that when the dc voltage control is empowered, regardless of whether the MPPT control is on or off and whether the PV power has changed or not, the dc voltage

V_{dc} is kept at 350 V. As an examination, when the dc voltage control is incapacitated and the MPPT control is off, when the PV power is liable to a change, the PV voltage will shift. Since the MPPT control is off, the obligation cycle proportion D_{st} is kept steady and the dc voltage V_{dc} shifts as well. This contextual investigation demonstrates that the dc voltage control in the vector control gives an extra measure to keep the dc voltage consistent.

C. Case 3: Performance of reactive power control

Another bit leeway of the three-stage HBC control is that it can bolster the air conditioner lattice by providing or retaining responsive power. The vector controller of PV charging station utilizing three-stage HBC is all around structured in past areas to accomplish decouple controlling without a doubt responsive power. This component connected for this situation concentrate to explore the capacity of the vector controller to rapidly follow the responsive power reference just as keep up a consistent dc voltage. The framework is first in enduring state and the vector controller directs the dc voltage and supply air conditioning power at solidarity power factor as appeared in Fig. 16. At $t=0.5$ seconds the reference receptive power assimilates 10 kVAr while at $t=1$ seconds it is changed to supply 20 kVAr to the primary air conditioning framework. The controller demonstrates a decent exhibition to follow the receptive power reference just as manage the dc voltage at 350 V. Fig. 16 outlines that the vector controller's M_d and M_q respond to the responsive power variety

just as primary a consistent dc voltage. It likewise demonstrates that the dc voltage and receptive power can be controlled autonomously.

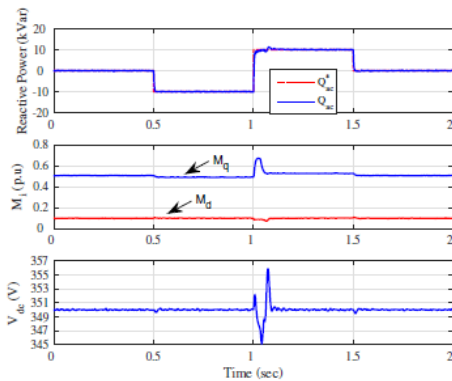
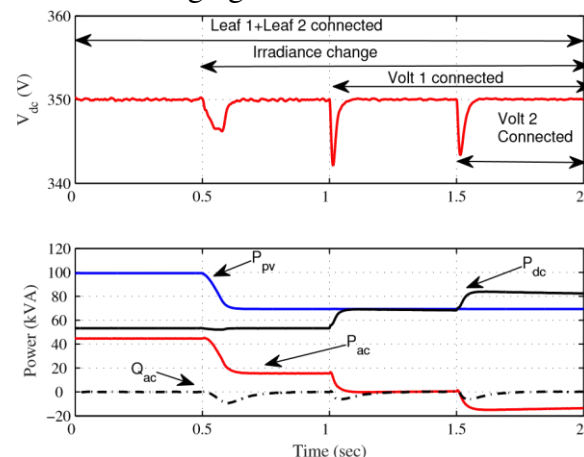


Fig. 16. Performance of a proposed vector control to supply or absorb reactive power independently.

D. Case4: Power management of the PV charging station

A target of the three-stage HBC is to charge PHEVs notwithstanding when there isn't sufficient PV control. The exhibition of the PV charging station is assessed when various estimations sun oriented illumination connected. The primary objective of this contextual investigation is to indicate nonstop charging PHEVs notwithstanding when the PV power is low. At daytime the sun oriented irradiance is thought to be 1 kW/m² while at sun set the irradiance diminishes to 0.7 kW/m². The dc load initially expends 50 kWh which speaks to charging of two Nissan Leaf vehicles. The two Nissan Leafs are charged before the PV power diminishes as appeared in Fig. 17. The staying of PV power moves to the fundamental matrix. At t=0.5 seconds, the PV power lessens because of irradiance change. Two additional vehicles are associated with the framework thusly at t=1 second and t=

1.5 seconds. Fig. 17 demonstrates that the PV exhibit can give capacity to the third vehicle at t = 1.5 seconds. The PV power is utilized to charge the batteries of PHEV with no reliance on the primary lattice. At t=1.5 seconds, the fourth electric vehicle is associated with the framework. The bidirectional element of the three-phase HBC and the managed dc voltage controller permit the dc burden to retain control from the principle network to charge the fourth vehicle as appeared in Fig. 16. It is additionally seen that the three-phase HBC can accomplish power balance just as keep up consistent dc voltage at 350 V. Fig. 17 additionally demonstrates that the responsive power Q_{ac} is kept at 0. This demonstrates the three-stage HBC can accomplish decoupled control of genuine and responsive power. Fig. 18 displays the obligation cycle proportion and the tweak file in dq-tomahawks. Fig. 19 exhibits the point by point control signals for adjusted PWM and the subsequent exchanging sequences. This contextual investigation shows that the proposed control can give smooth change when HPEVs are associated into the PV charging station.



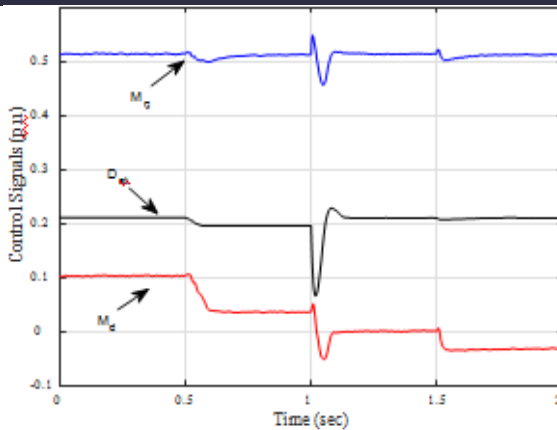


Fig. 18. M_d , M_q and M_c for case 4.

E. Case5: Partial grid failure

The controller structure of the three-stage HBC based PV charging station can deal with the incomplete matrix disappointment. The controller is intended to give a steady dc voltage notwithstanding when framework shortcoming is happened. For the most part, when the primary framework voltages sag beneath 80% of the ostensible voltage, the power quality models prescribe to detach the charged PHEV to secure the battery's life cycle [37]. The objective of planning the PV charging station's controller is to accomplish consistent charging methodology when a deficiency is happening at the primary network. The strategy for is to give adequate capacity to charge the PHEV's batteries just as to keep up a consistent dc-connect voltage. Subsequently, it is pointless to disengage the PHEVs during framework deficiency. The capacity of halfway framework disappointment resilience is exhibited in the accompanying contextual analysis. The PV charging station is first associated with the principle lattice where the PHEV's batteries are charged during the relentless state period. MPPT is empowered

at $t = 0.5$ seconds. A symmetrical 70% voltage droop is happened at $t = 1.0$ seconds. Regularly, it is prescribed to detach the air conditioner load just as the PHEV's batteries for security and wellbeing. In any case, the proposed controller can alleviate this issue by balancing out the dc-interface voltage at its evaluated an incentive just as creating the expected capacity to the neighborhood air conditioning load. As can be found in Fig. 20, the controller of the PV charging station can balance out the dc transport voltage at its appraised worth. As appeared in Fig. 20, the produced genuine power from the PV station (P_{pv}) is kept the equivalent (100 kW) due to MPPT control. The PHEV load (60 kW) is kept the equivalent since the dc-transport voltage is kept the equivalent. Thus, the power directly after the HBC PHBC to the air conditioner side is kept the equivalent (40 kW). The 70% decrease in the air conditioner voltage diminishes the heap control utilization from 20 kW to diminished to 10 kW. Thusly, the ability to the network P_{ac} is expanded to 30 kW. At $t = 1.5$ seconds, the voltage recoups to 1 pu and the forces come back to the qualities before 1 seconds.

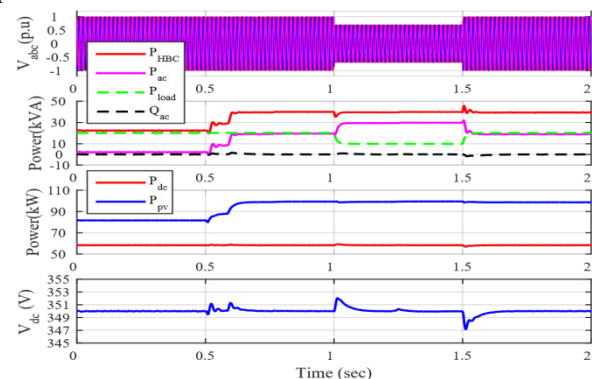


Fig. 20. System performance under 70% grid's voltage drop.

V. EXPERIMENTAL RESULTS

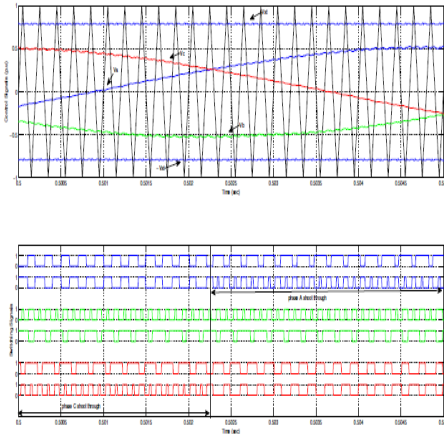


Fig. 19. The modified PWM signals and the switching sequences.

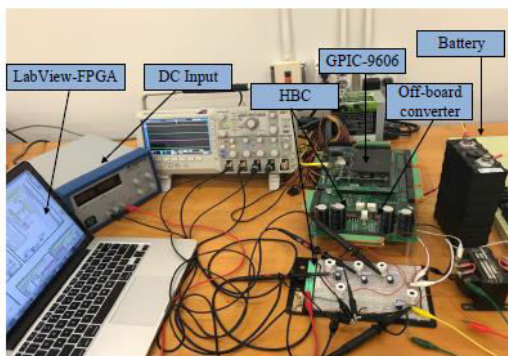


Fig. 21. Experimental setup for laboratory prototype of the charging station.

The conduct of the proposed PHEV charging station has been approved utilizing a research center model. National Instruments (NI) Single-Board RIO-9606 and a NI General Purpose Inverter Controller (GPIC) are utilized to approve the topology of the HBC-based PV charging station. The LabViewfieldprogrammable door cluster (FPGA) performs sign preparing, information investigation, and framework controlling utilizing a host PC. The framework's controller is executed utilizing LabView-FPGA to drive the switches of the HBC just as screen the charging strategy of the battery. It likewise

gives a framework's assurance by checking the warm conduct of the HBC just as disengaging the battery when a shortcoming happens. NI-GPIC load up measures the ongoing information of the power inverter and executes the controlling sign. The traded data security reasons, the power rating is downscaled because of the restriction of the genuine battery and the NI-GPIC. Fig. 21 demonstrates the lab arrangement of the PHEV charging station. The design of the exploratory testing is arranged into five principle parts, including NI Single-Board GPIC RIO-9606, NIGPIC back-back inverters, a host LabView-FPGA PC, dc power supply, and dc and air conditioning loads. The NI-GPIC back-back inverters contain two inverters which are utilized for the HBC topology and off-board dc/dc converter. The arrangement of the HBC requires changing the topology of the NI-GPIC backback inverters since the exploration board contains just threephase IGBT-based inverters. The point by point setups of the

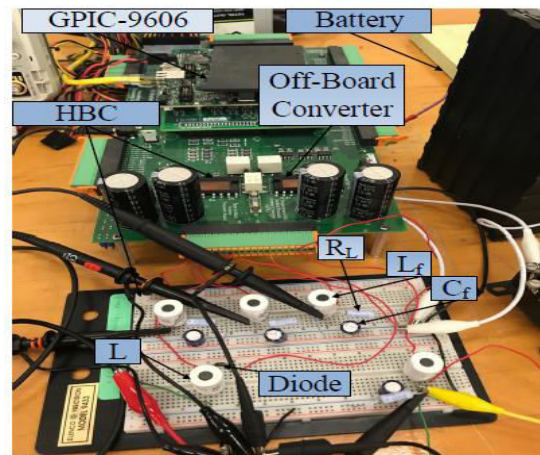


Fig. 22. Detailed laboratory configuration of the HBC and off/board converter.

HBC and off-board converters are given in Fig. 22. The dc burden contains Lithium-particle battery which mirrors the PHEV's battery. Sinopoly SP-LFP40AHA Lithium-particle battery is utilized for the trial testing which is associated with the offboard dc/dc converter for playing out a charging methodology. The programmable dc source is utilized for supplanting the PV power source. The air conditioner yield channel contains LC parts to filter out the high-recurrence segments of the yield signals.

TABLE II
PARAMETERS OF THE LABORATORY PHEV CHARGER.

System Parameters AC side	Value	System Parameters DC side	Value
AC frequency	377 rad/second	V_{pv}	10 V
HBC F_{sw}	5 kHz	DC/DC F_{sw}	10 kHz
L_f	5.6 mH	DC-link voltage	20 V
C_f	47 μ F	C_{pv}	47 μ F
V_{ac}	5V _{peak}	L	5.6 mH
R_L	30 Ω	Li-ion Voltage	3.2 V
K_{pdc}	0.5	K_{idc}	0.001

The air conditioner side is associated with a resistive burden R_L . The rundown of parameters and downscaled estimations of the research center PHEV charger are given in Table. II. The control plan of the HBC-based PV charging station has been connected in Lab View-FPGA to drive the switches of the HBC. A shut circle control for Vdc is utilized to control the dc transport voltage by directing the Dstas given in Fig. 23.

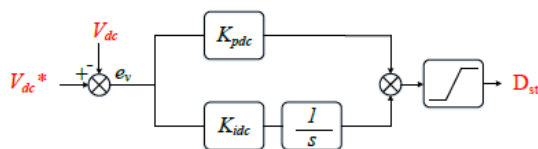


Fig. 23. Closed-loop control for dc bus voltage. $K_{pdc} = 0.5$, $K_{idc} = 0.001$.

The controlled sign Dstis then connected to the adjusted PWM to characterize the shoot-through period. The dc info source can produce both dc and air conditioning

force yields. Fig. 24 demonstrates the unflinching state yield waveforms from a solitary information dc source. The three-stage air conditioning yields are sustained to a three-stage adjusted burden while the dc power is utilized to charge the battery at the dc transport. Fig. 24 demonstrates that the information 10 V dc can produce 20 V dc and 5 V pinnacle for every stage voltage V_{abc} when $D_{standMi}$ are 0.5 and 0.25, individually. It tends to be seen that the summation of $D_{standMi}$ is under 1, which fulfills the activity of the altered PWM.

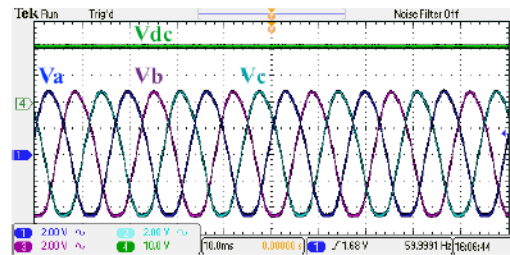


Fig. 24. Steady state output waveforms for HBC. The V_{dc} equals 20 V at while the value of D_{st} equals 0.5. The peak phase V_{abc} equals 5 V at 0.25 of M_i .

As indicated by (2), the pinnacle per-stage air conditioning voltage relies upon both $D_{standMi}$. Figs. 25 and 26 demonstrate a stage change in the yield dc voltage from 1 V to 20 V prompting an expansion in the D_{stas} well as an increment in the yield air conditioning voltage. The yield signal D_{st} from the Vdc shut circle controller changes from 0.33 to 0.5 (appeared in Fig. 25) while the estimation of M_i keeps consistent. Fig. 27 demonstrates the conduct of stage a when a stage change in the M_i is connected from 0.2 to 0.25 which prompts change the V_{ac} from 4 to 5 V while the dc-interface voltage stays steady as 20 V. As prosecuted by (1), managing M_i prompts change in the air conditioner yield voltage however not in

dc yield voltage. Figs. 26 and 27 check (1) and (2).

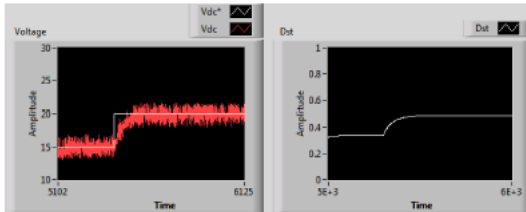


Fig. 25. Performance of closed-loop voltage using LabView-FPGA when the reference V_{dc} is changed from 15 V to 20 V.

VI. CONCLUSION

Control of three-stage HBC in a PV charging station is proposed in this paper. The three-stage HBC can be extended by adding a dc/dc converter and a cooling converter into a single converter structure. Another control for the three-stage HBC is proposed to achieve MPPT, dc voltage regulation and responsive power following. The MPPT control uses an adjusted conductance-PID based MPPT methodology. The dc voltage regulation and responsive power following are recognized using vector control. Five relevant examinations are driven in PC simulation to demonstrate the performance of MPPT, dc voltage regulation, open power following and by and large control the administrators of the PV charging station. Preliminary outcomes affirm the action of the PHEV charging station using HBC topology. The reenactment and exploratory results show the feasibility and quality of the proposed control for PV energizing station to keep constant dc power supply using both PV power and cooling network control.

REFERENCES

1. M. Ehsani, Y. Gao, and A. Emadi, Modern electric, cross breed electric, and

energy unit vehicles: essentials, hypothesis, and structure. CRC press, 2009.

2. K. Sikes, T. Net, Z. Lin, J. Sullivan, T. Cleary, and J. Ward, "Module cross breed electric vehicle advertise presentation study: last report," Oak Ridge National Laboratory (ORNL), Tech. Rep., 2010.

3. Fig. 26. A stage change on the dc voltage. V_{dc} is changed from 15 V to 20 V which prompts alter the D_{st} from 0.33 to 0.5. The pinnacle V_a is additionally expanded from 4 V to 5 V on account of V_{dc} variety. The estimation of the M_i stays steady at 0.25 during the V_{dc} step change.

4. Khaligh and S. Dusmez, "Extensive topological investigation of conductive and inductive charging answers for module electric vehicles," IEEE Transactions on Vehicular Technology, vol. 61, no. 8, pp. 3475–3489, 2012.

5. T. Anegawa, "Advancement of brisk charging framework for electric vehicle," Tokyo Electric Power Company, 2010.

6. F. Musavi, M. Edington, W. Eberle, and W. G. Dunford, "Assessment and effectiveness examination of front end air conditioning dc module half and half charger topologies," IEEE Transactions on Smart lattice, vol. 3, no. 1, pp. 413–421, 2012.

7. M. Yilmaz and P. T. Krein, "Survey of battery charger topologies, charging force levels, and foundation for module electric and half and half vehicles," IEEE Transactions on Power Electronics, vol. 28, no. 5, pp. 2151–2169, May 2013.

8. G. Gamboa, C. Hamilton, R. Kerley, S. Elmes, A. Arias, J. Shen, and I. Batarseh,



"Control procedure of a multi-port, matrix associated, direct-dc pv charging station for module electric vehicles," in Energy Conversion Congress and Exposition (ECCE), 2010 IEEE. IEEE, 2010, pp. 1173–1177.

9. P. Goli and W. Shireen, "Pv incorporated brilliant charging of phevs dependent on dc interface voltage detecting," IEEE Transactions on Smart Grid, vol. 5, no. 3, pp. 1421–1428, 2014.

10. S. Mishra, R. Adda, and A. Joshi, "Opposite watkins–johnsontopologybased inverter," IEEE Transactions on Power Electronics, vol. 27, no. 3, pp. 1066–1070, 2012.

11. O. Beam and S. Mishra, "Lift determined mixture converter with

synchronous dc and air conditioning yields," IEEE Transactions on Industry Applications, vol. 50, no. 2, pp. 1082–1093, March 2014.

12. Fig. 27. A stage change on the M_i . The yield crest V^{abc} is changed from 4 V to 5 V by differing the M_i from 0.2 to 0.25. The V_{dc} stays steady when a stage change at 20 V. The estimation of the D_{st} keeps fixed at 0.5 during the variety of M_i .